Performance Analysis of the Maximum Ratio Transmission Preprocessing for Extended Receive Antenna Shift Keying

Ali Mokh, Matthieu Crussière, Maryline Hélard

Performance Analysis of the Maximum Ratio Transmission Preprocessing for Extended Receive Antenna Shift Keying

Ali Mokh, Matthieu Crussière, Maryline Hélard
Univ Rennes, INSA Rennes, IETR, CNRS, UMR 6164, F-35000 Rennes

***Abstract*—The Extended Receive Antenna Shift Keying (ERASK) scheme is a MIMO scheme based on the Receive Spatial Modulation concept, invented to increase the overall spectral efficiency, by exploiting all possible combinations of receive antenna indexes. In this paper, we evaluated the ERASK scheme using the Maximum Ratio Transmission (MRT) preprocessing (MRT-ERASK), using the real amplitude threshold detector and compare it with the ERASK scheme using the Zero Forcing (ZF) preprocessing (ZF-ERASK). Analytical derivations of the received signal of the MRT-ERASK show that a complex inter-antenna interference is added to other antennas depending on the transmitted spatial symbol. The Bit Error Rate performance is also derived analytically. Simulation results over MIMO Rayleigh channel are provided to compare both systems, showing that ZF-ERASK outperforms MRT-ERASK but at the expense of a higher implementation complexity for ZF-ERASK. On the other hand, increasing the number of transmit antennas of a MRT-ERASK improves its performance getting closer to the performance ZF-ERASK. Therefore, the higher the number of transmit antennas, the nearer the performance of both systems, and the more suitable the MRT-ERASK to be implemented.**

***Index Terms*—Extended Receive Antenna Shift Keying, MIMO, Spatial Modulation, Zero Forcing, Maximum Ratio Transmission, Spatial Modulation.**

I. Introduction

Space Modulation is a Multiple-Input and Multiple-Output (MIMO) based scheme appeared in the early 2000s in the name of Space Shift Keying (SSK) [1] whose main principle is to take advantage of the various propagation characteristics associated to the different antennas of the system. Given a rich scattering environment, the receiver can utilize the distinct received signals from different antennas to discriminate between the transmitted information messages. This results in a simple SSK signal demodulation and then in cost-effective receiver structures. In conventional Spatial Modulation (SM), the concept of the SSK is applied but with the addition of the classical IQ-symbols [2][3].

Afterwards, a particular SM implementation case was proposed in [4] and referred to as Transmitter Preprocessing Aided Spatial Modulation (TPSM), where the spatial modulation concept is applied at the receiver side, joining conventional amplitude-phase modulation and preprocessing aided SSK (pre-SSK). The general concept of the spatial modulation was further applied at the receiver side in a so-called Receive-Spatial Modulation (RSM) [5]. RSM scheme is a combination of the Receive Antenna Shift Keying (RASK) [6], where only the index of the targeted receive antenna carries the spatial information, using a preprocessing technique to target the signal towards the RAs , and of IQ symbols.

A generalization of the RSM principle, further referred to as GPSM (Generalised Pre-coding aided Spatial Modulation), is proposed in [7] where the transmit antennas concentrate the signal energy towards a fixed and constant number of receive antennas to increase the spectral efficiency. In [8], an extended model of RASK is also presented, referred to as ERASK, where all combinations of different numbers of targeted antennas are used. The ZF preprocessing was employed, supposing a perfect channel estimation at the transmitter side. The scheme was proposed to be suitable for the low power consumption devices in the downlink because of the simple detection algorithm [9].

Maximum Ratio Transmission (MRT) and Time Reversal preprocessing can also be carried out enabling to focus a signal in both time and space[10][11]. Because of a channel state information at the transmitter side, and the possibility of the preprocessing in the time domain, all these schemes are suitable for Time Division Duplex (TDD) systems [12].

In this paper, the ERASK scheme with MRT preprocessing is evaluated. The equation of the received signal was derived to find the analytical performance using the same detection algorithm used in [8]. The ZF-ERASK is demonstrated to outperform the MRT-ERASK but at the expense of a higher complexity making MRT-ERASK more suitable for systems with high number of transmit antennas.

The rest of the paper is organized as follows. In Section II, we recall the principle of the ERASK scheme, and explain the transmission of a sequence of bits. In Section III, the system model and the block diagram of the ERASK scheme with MRT are detailed. In Section IV, theoretical computation of the *Bit Error Rate* is derived. Simulation results are provided in Section V, and a conclusion is drawn in Section VI.

II. ERASK Principle

In this section, we remind the ERASK principle, which is based on the SM concept at the receiver. In ERASK scheme, the number of targeted antennas N_a changes at each symbol duration T_s with $0 \leq N_a \leq N_r$, where N_r is the number of receive antennas, taking all possible values, depending on the information bits, so that the number M of possible spatial symbols achieves 2^{N_r} providing an ERASK symbol made of a

101 110 010 011	Symbol 1	Symbol 2	Symbol 3	Symbol 4
1) Segmentation	101	110	010	011
2) Mapping	R1&R3	R1&R2	R2	R2&R3
3) Preprocessing (focalisation)	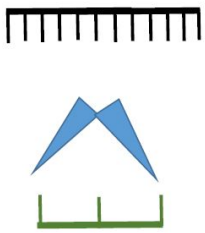	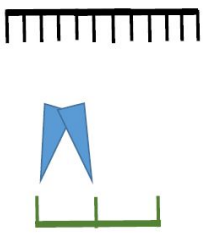	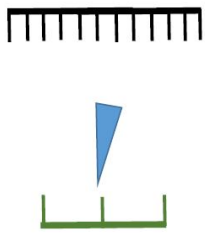	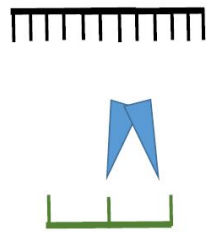
4) Detection	R1&R3	R1&R2	R2	R2&R3
5) Demapping	101	110	010	011

Figure 1. The concept of binary sequence transmission with ERASK scheme where $N_r = 3$

number $m = N_r$ of bits. Fig. 2 provides an example illustrating the transmission of a binary sequence, using the ERASK concept with 3 receive antennas. Steps 1 and 2 allow for forming M-ary spatial symbol with $M = 8$ and transmitting 3 bits during each T_s. In the first symbol, a group of bits "101" is mapped to a spatial symbol that allows to target the two receive antennas R_1 and R_3. Hence, at step 3, the preprocessing is performed at the transmitter so as to create a beam to concentrate the transmitted energy towards the N_a targeted antennas. At step 4, the receiver estimates which antennas have been targetted by analyzing the received signal at the receive antennas, and then deduces the transmitted spatial symbol. In [8], a Zero-forcing preprocessing was performed so that no signal at all was received on the non-targetted antenna, i.e. cancelling interfences at the receiver . A Maximum Likelihood based detector was therefore reduced to a simple threshold.

III. System model

A MIMO system with N_t transmit antennas and N_r receive antennas is considered. Assuming a MIMO channel operating on Rayleigh fading, between the transmitter and the receiver, the receive signal vector can be written as:

$$\mathbf{Y} = \mathbf{H}\ \mathbf{S} + \mathbf{N} \tag{1}$$

where $\mathbf{Y} \in \mathbb{C}^{N_r \times 1}$ is the vector of the received signals on all receive antennas, $\mathbf{H} \in \mathbb{C}^{N_r \times N_t}$ is the MIMO channel matrix with elements $h_{j,i}$ representing the complex channel coefficient between the i-th transmission antenna, denoted by T_i, and the j-th receiving antenna, denoted by R_j. $\mathbf{S} \in \mathbb{C}^{N_t \times 1}$ is the vector of the transmitted symbol with normalized energy, and $\mathbf{N} \in \mathbb{C}^{N_r \times 1}$ is the vector of additive white Gaussian noise (AWGN) samples η_j such that $\eta_j \sim \mathcal{CN}(0, \sigma_n^2)$.

The block diagram of the ERASK system is depicted in Fig. 2. A group of $m = N_r$ bits is mapped to a spatial symbol $\mathbf{X}_k \in \mathbb{N}^{N_r \times 1}$ which is written as

$$\mathbf{X}_k = \begin{bmatrix} x_1(k) & x_2(k) & \dots & x_{N_r}(k) \end{bmatrix}^T \text{ where } x_j(k) \in \{0, 1\}.$$

Since in ERASK scheme, all spatial combinations are possible, so $k \in [1, 2^{N_r}]$. The value taken by each $x_j(k)$ entry determines the set of targeted receive antennas such that:

$$x_j = \begin{cases} 0, & \text{if } R_j \text{ is not targeted,} \\ 1, & \text{if } R_j \text{ is targeted.} \end{cases} \tag{2}$$

Then, the pre-processing block transforms the vector of spatial symbols $\mathbf{X}_k$ into a vector of transmitted signals denoted by $\mathbf{S} \in \mathbb{C}^{N_t \times 1}$ using the pre-processing matrix $\mathbf{W} \in \mathbb{C}^{N_t \times N_r}$. In this paper, the MRT is employed for the pre-processing step, where in the frequency domain, the trans-conjugate of the channel matrix is used as a pre-filter:

$$\mathbf{W} = \mathbf{H}^H. \tag{3}$$

The technique aims to increase the Signal-to-Noise Ratio SNR on the receive antennas, and can be implemented easily in the time domain as the "Time Reversal" preprocessing [6]. As for different schemes based on the RSM concept, a channel estimation at the transmitter is required for the pre-processing block. Consequently, the transmitted signal is written as:

$$\mathbf{S} = f\ \mathbf{W}\ \mathbf{X}_k = f\ \mathbf{H}^H \mathbf{X}_k \tag{4}$$

where f is a normalization factor used to guarantee that the average total transmit power $\bar{P}_t$ is equal to 1. More precisely we have,

$$f = \frac{1}{\sqrt{\mathbb{E}_x\{\mathrm{Tr}(\mathbf{W}\ \mathbf{X}\ \mathbf{X}^H\ \mathbf{W}^H)\}}} = \frac{1}{\sqrt{\sigma_x^2 \mathrm{Tr}(\mathbf{H}^H\ \mathbf{H})}} \tag{5}$$

where $\mathrm{Tr}(.)$ holds for the trace of matrix and $\mathbb{E}_x$ stands for the expectation over x. Since $\mathbf{X}$ has i.i.d. entries, the variance

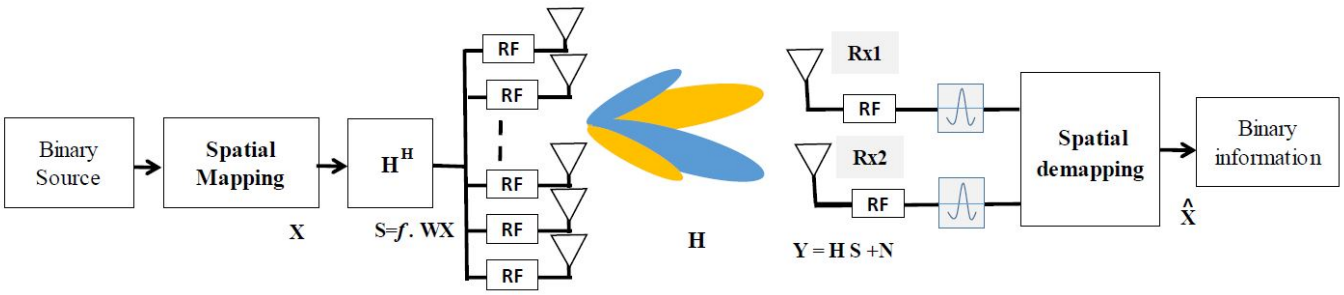

Figure 2. Block diagram of Extended-RASK

$\sigma_x^2 = \mathbb{E}_x\left[x_j x_j^*\right]$ is independent of j and comes in factor of the trace computation. Then, each entry of $\mathbf{X}$ is of amplitude 1 with a probability $\frac{1}{2}$, leading to $\sigma_x^2 = \frac{1}{2}$.

However, unlike the Zero-Forcing preprocessing used in [8] where the required number of antennas should satisfy the constraint $N_r \leq N_t$ so that the matrix inversion remains possible, for MRT processing, it is straightforward to obtain the expression of the receive signals:

$$\mathbf{Y} = f\ \mathbf{H}\ \mathbf{H}^H.\ \mathbf{X}_k + \mathbf{N}. \tag{6}$$

without any pseudo inverse channel matrix computation.

At the level of the received antenna R_j, the received signal then writes:

$$\begin{aligned} &y_j(k) = \\ &f\left(\sum_{i=1}^{N_t}\|h_{j,i}\|^2 \times x_j(k) + \sum_{i=1}^{N_t}\sum_{l=1,l\neq j}^{N_r} h_{j,i}h_{i,l}^* x_l(k)\right) + \eta_j \\ &= \beta_j \times x_j(k) + I_j(k) + \eta_j. \end{aligned} \tag{7}$$

where

$$\beta_j = f\sum_{i=1}^{N_t}\|h_{j,i}\|^2$$

is the amplitude of the focused signal toward antenna R_j, and

$$I_j(k) = f\sum_{i=1}^{N_t}\sum_{l=1,l\neq j}^{N_r} h_{j,i}h_{i,l}^* x_l(k)$$

is the additional interference to the antenna R_j when sending the spatial symbol $\mathbf{X}_k$. It is shown that the focused signal $x_j(k)$ is multiplied by a real amplitude, while a complex interference is added to the received signal depending on the spatial symbol, specifically the entries of $\mathbf{X}$ that are referred to other receive antennas.

IV. Detection and Analytical Performance

A. Detection

To estimate the spatial symbol, the receiver should detect whether each receive antenna is targeted by the transmitter or not. The *Real Amplitude Threshold* detector used in [8] for ZF-ERASK will be used in this paper as detector for MRT-ERASK. The so-called *Real Amplitude Threshold* detector consists in fact in detecting which received signal has a real part greater than a given threshold [8]. Notice that this detector is equivalent to the Maximum Likelihood detector for a ZF-ERASK system, but here with MRT preprocessing it is not the case because of interference at the non targetted antennas. Detecting if antenna R_j is targetted will therefore be obtained by:

$$\hat{x}_j(k) = \begin{cases} 0, & \text{if } \Re\{y_j\} \leq \nu_j, \\ 1, & \text{if } \Re\{y_j\} \geq \nu_j. \end{cases} \tag{8}$$

where ν_j is a predefined amplitude threshold at the antenna R_j. From Eq. (7), a given detector has to analyze the following set of signals:

$$\forall j, \quad y_j(k) = \begin{cases} \beta_j + I_j(k) + \eta_j & \text{if } R_j \text{ is targeted} \\ I_j(k) + \eta_j & \text{otherwise} \end{cases} \tag{9}$$

The interference factor $I_j(K)$ changes between different values depending on the spatial symbol, between a minimum value where all other antennas are not targeted, and a maximum value where all other antennas are targeted:

$$\min_K(I_j) = 0$$

$$\max_K(I_j) = f\sum_{i=1}^{N_t}\sum_{l=1,l\neq j}^{N_r} h_{j,i}h_{i,l}^*.$$

From Eq. (9), we can define ν_j as:

$$\nu_j = \frac{\beta_j + \Re\{\max_k(I_j)\}}{2}. \tag{10}$$

B. Analytical Performance

In this section, we are deriving the analytical approach for the BER performance of the ERASK system employing MRT preprocessing. The formula that derives the analytic BER $\mathcal{P}_e$ is:

$$\mathcal{P}_e = \frac{1}{m}\cdot\mathbb{E}\left\{\sum_{k}^{N_r}\sum_{j\neq i}^{N_r}\mathcal{P}(\mathbf{X}_k \to \mathbf{X}_j)\cdot d(\mathbf{X}_k, \mathbf{X}_j)\right\}. \tag{11}$$

where $d(\mathbf{X}_k, \mathbf{X}_j)$ is the Hamming distance between two spatial symbols $\mathbf{X}_k$ and $\mathbf{X}_j$, and $\mathcal{P}(\mathbf{X}_k \to \mathbf{X}_j)$ is the probability to

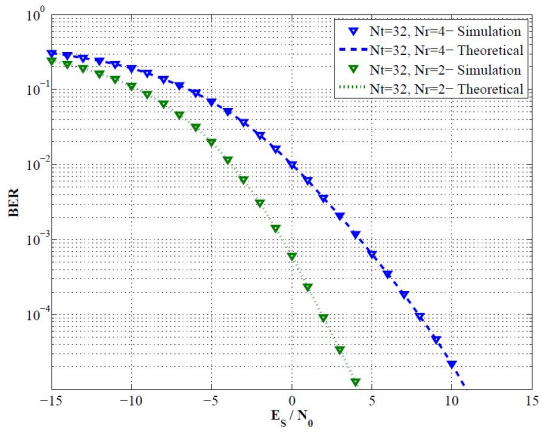

Figure 3. BER performance of two MRT-ERASK over Rayleigh fading channel, N_t= 32, N_r=2 and 4, simulation and theoretical results

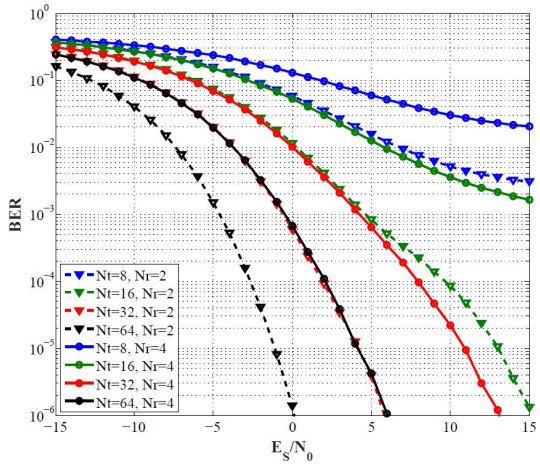

Figure 4. Comparison of the BER performance of two MRT-ERASK over Rayleigh fading channel, N_r=2 and 4

transmit X_k and detect X_j. All spatial signatures are possible and equally likely in ERASK scheme, and so for each receive antenna, the probability of being targeted or not is independent on all other receive antennas. Using a threshold detector in parallel on each receive antenna leads to evaluate the BER on each antenna. Define as the probability $\mathcal{P}(y_{j1})$ (resp. $\mathcal{P}(y_{j0})$) that one particular antenna R_j is targeted (resp. not targeted). Since $x_k \in \{0, A\}$ with a probability of $\frac{1}{2}$, then $\mathcal{P}(y_{j0}) = \mathcal{P}(y_{j1}) = \frac{1}{2}$, we have:

$$\mathcal{P}_e = \frac{1}{2} \cdot \mathcal{P}(y_{j0} \to y_{j1}) + \frac{1}{2} \cdot \mathcal{P}(y_{j1} \to y_{j0}). \tag{12}$$

Then, applying the threshold detection, let $\mathcal{P}_e(k)$ be the probability of error when sending spatial symbol $\mathbf{X}_K$. We obtain:

$$\begin{aligned} \mathcal{P}_e(k) = \frac{1}{2} \times \Big[& \mathcal{P}\left(\nu_j \leq \Re\{I_j(K) + \eta_j\}\right) \\ & + \mathcal{P}\left(\Re\{\beta_j + I_j(K) + \eta_j\} \leq \nu_j\right) \Big] \end{aligned} \tag{13}$$

Since noise samples are centered circularly Gaussian of variance σ_n^2, we finally get:

$$\begin{aligned} \mathcal{P}_e(k) =& \mathcal{P}\left(\mathcal{N}(0, \frac{\sigma_n^2}{2}) \geq \nu_j - \Re\{I_j(K)\}\right) \\ =& Q\left(\frac{\nu_j - \Re\{I_j(K)\}}{\sigma_n/\sqrt{2}}\right). \end{aligned} \tag{14}$$

where $Q(.)$ denotes the Gaussian Q-function. As a result, the general equation of the BER is given as:

$$\mathcal{P}_e = \frac{1}{N_r 2^{N_r}} \sum_{j=1}^{N_r} \sum_{K=1}^{2^{N_r}} Q\left(\frac{\beta_j + \Re\{\max_k(I_j)\} - 2\Re\{I_j(K)\}}{\sigma_n \sqrt{2}}\right). \tag{15}$$

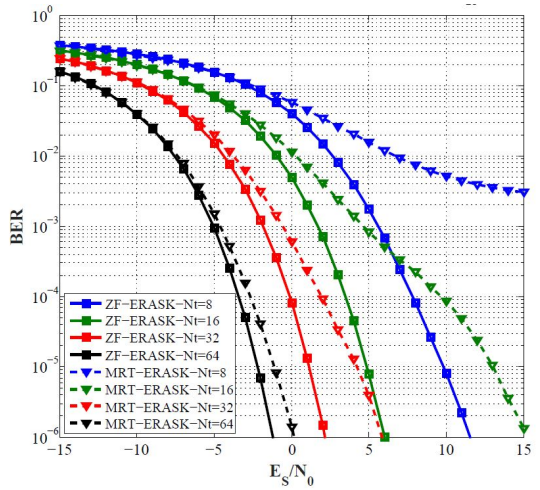

Figure 5. Comparison of the BER performance of MRT-ERASK and ZF-ERASK over Rayleigh fading channel, N_r=2

V. Simulation Results

In this section, BER performance are provided versus the ratio between the average of the symbol energy and the noise spectral density of the ERASK system:

$$\frac{E_S}{N_0} = \frac{1}{\sigma_n^2}.$$

It is assumed that $\mathbf{H}$ is a MIMO flat fading channel matrix where $h_{j,i}$ are complex coefficients following i.i.d. Rayleigh distribution. The power for each sub-channel is normalized:

$$E\left[\, \|h_{j,i}\|^2 \,\right] = 1.$$

Finally, we consider that the channel response is perfectly known at the transmitter. Simulations are run by implementing a sufficient number of iterations for different channel realizations, and taking the mean value of the BER for each value of $\frac{E_S}{N_0}$. In all simulations, the receiver uses the Real Amplitude Threshold Detection to estimate the spatial symbol.

In Fig. 3, we compare the simulation results with the theoretical results provided by the derivation of the theoretical analysis of the BER. Two MRT-ERASK with $N_t = 32$ TAs and with $N_r = 2$ and 4 are provided. Results obviously show that the simulation results perfectly match with the theoretical derivation. In Fig. 4, simulation results are presented considering an ERASK system with $N_t = 8$, 16, 32 and 64, and with $N_r = 2$ and 4. The results first show that for a given number of receive antennas, the higher the number of transmit antennas, the better the performance due to a better focusing gain and a lower interference level towards the non targeted antennas [13]. As also evident from this figure, the higher the order of the spatial modulation, i.e. the number of receive antennas N_r, the greater the performance degradation. Indeed, as N_r increases, the trace $\mathbf{H}^H\mathbf{H}$ that is proportional to N_r also increases, and so the normalization factor f that controls the signal amplitude of the received signal in Eq. (7) decreases.

In Fig. 5, we are considering ERASK systems with $N_r = 2$, and with $N_t = 8$, 16, 32 and 64. The ZF and the MRT preprocessing are employed and compared for all system configurations. As evident from the obtained curves, the higher N_t, the better the performance of the two systems. This result was approved in [8], and here is verified also with the MRT preprocessing. Also, for all system configurations, the ZF-ERASK outperforms the MRT-ERASK, because of the interference cancellation. Nevertheless, the difference in performance decreases when increasing the number of transmit antennas, which makes the MRT-ERASK more suitable because of the lower implementation complexity compared to the Zero-Forcing system that requires a matrix inversion.

VI. Conclusion

In this paper, performance of an ERASK scheme using the Maximum Ratio Transmission (MRT) preprocessing was analytically provided when using a real amplitude threshold detector. Analytical derivations of the received signal of the MRT-ERASK show that a complex inter-antenna interference is added to other antennas depending on the spatial symbol. A performance comparison with an ERASK scheme using the Zero Forcing (ZF) preprocessing (ZF-ERASK) was also carried out. Simulations results over MIMO Rayleigh channel are provided to compare both systems, showing that ZF-ERASK outperforms MRT-ERASK but at the expense of a higher implementation complexity for ZF-ERASK due channel matrix inversion. Nevertheless, increasing the number of transmit antennas of a MRT-ERASK improves its performance getting closer to the ZF-ERASK performance. Therefore, the higher the number of transmit antennas, the nearer the performance of both systems, and the more suitable the MRT-ERASK to be implemented.

Acknowledgment

The authors would like to thank the SPATIAL MODULATION project funded by the French National Research Agency (ANR)

References

[1] Y. A. Chau and S.-H. Yu, 'Space modulation on wireless fading channels', in *Vehicular Technology Conference, 2001. VTC 2001 Fall. IEEE VTS 54th*, IEEE, vol. 3, 2001, pp. 1668–1671.

[2] R. Y. Mesleh, H. Haas, S. Sinanovic, C. W. Ahn, and S. Yun, 'Spatial modulation', *IEEE Transactions on Vehicular Technology*, vol. 57, no. 4, pp. 2228–2241, 2008.

[3] M. Di Renzo, H. Haas, A. Ghrayeb, S. Sugiura, and L. Hanzo, 'Spatial modulation for generalized MIMO: Challenges, opportunities, and implementation', *Proceedings of the IEEE*, vol. 102, no. 1, pp. 56–103, 2014.

[4] L.-L. Yang, 'Transmitter preprocessing aided spatial modulation for multiple-input multiple-output systems', in *Vehicular Technology Conference (VTC Spring), 2011 IEEE 73rd*, IEEE, 2011, pp. 1–5.

[5] A. Stavridis, S. Sinanovic, M. Di Renzo, and H. Haas, 'Transmit precoding for receive spatial modulation using imperfect channel knowledge', in *Vehicular Technology Conference (VTC Spring), 2012 IEEE 75th*, IEEE, 2012, pp. 1–5.

[6] D.-T. Phan-Huy and M. Hélard, 'Receive antenna shift keying for time reversal wireless communications', in *2012 IEEE International Conference on Communications (ICC)*, IEEE, 2012, pp. 4852–4856.

[7] R. Zhang, L.-L. Yang, and L. Hanzo, 'Generalised precoding aided spatial modulation', *IEEE Transactions on Wireless Communications*, vol. 12, no. 11, pp. 5434–5443, 2013.

[8] A. Mokh, M. Hélard, and M. Crussière, 'Extended receive antenna shift keying', in *2017 IEEE International Conference on Telecommunication (ICT)*, IEEE, 2017.

[9] A. MOKH, M. Hélard, and M. Crussière, 'Space shift keying modulations for low complexity internet-of-things devices', in *2017 IEEE Global Communications Conference (GLOBCOM)*, IEEE, 2017.

[10] Y. Kokar, J.-C. Prevotet, and M. Helard, 'Receive antenna shift keying modulation testbed for wireless communications systems', in *Globecom Workshops (GC Wkshps), 2016 IEEE*, IEEE, 2016, pp. 1–6.

[11] A. Mokh, Y. Kokar, M. Hélard, and M. Crussière, 'Time Reversal Receive Antenna Shift Keying on MIMO LOS channel', in *2017 International Conference on Sensors, Networks, Smart and Emerging Technologies (SENSET)*, IEEE, 2017.

[12] A. Derode, P. Roux, and M. Fink, 'Robust acoustic time reversal with high-order multiple scattering', *Physical review letters*, vol. 75, no. 23, p. 4206, 1995.

[13] F. Rusek, D. Persson, B. K. Lau, E. Larsson, T. Marzetta, O. Edfors, and F. Tufvesson, 'Scaling Up MIMO: Opportunities and Challenges with Very Large Arrays', *IEEE Signal Processing Magazine*, vol. 30, no. 1, pp. 40–60, Jan. 2013, ISSN: 1053-5888.